Air pollution and climate forcing of the charcoal industry in Africa

Alfred S. Bockarie[a], Eloise A. Marais[b§*], A. R. MacKenzie[a,c]

[a] School of Geography, Earth and Environmental Sciences, University of Birmingham, Birmingham, UK

[b] School of Physics and Astronomy, University of Leicester, Leicester, UK

[c] Birmingham Institute of Forest Research, University of Birmingham, Birmingham, UK

[§] Now at: Department of Geography, University College London, London, UK

ABSTRACT

Demand for charcoal in Africa is growing rapidly, driven by urbanization and lack of access to electricity. Charcoal production and use, including plastic burning to initiate combustion, release large quantities of trace gases and particles that impact air quality and climate. Here we develop an inventory of current (2014) and future (2030) emissions from the charcoal supply chain in Africa that we implement in the GEOS-Chem model to quantify the contribution of charcoal to surface concentrations of $PM_{2.5}$ and ozone, and direct radiative forcing due to aerosols and ozone. We estimate that the charcoal industry in 2014 required 140-460 Tg biomass and 260 tonnes plastic and that industry emissions could double by 2030, so that charcoal industry methane emissions could outcompete those from open fires by 2025. In 2014, the largest enhancements in $PM_{2.5}$ (0.5-1.4 μg m^{-3}) and ozone (0.4-0.7 ppbv) occur around densely populated cities in East and West Africa. Cooling due to aerosols (-100 to -300 mW m^{-2}) is concentrated over dense cities, whereas warming due to ozone is widespread, peaking at 4.2 mW m^{-2} over the Atlantic Ocean. These effects will worsen with ongoing dependence on this energy source, spurred by rapid urbanization and absence of viable cleaner alternatives.

Keywords: Biomass, emissions, air quality, climate, chemical transport model

Abstract Art

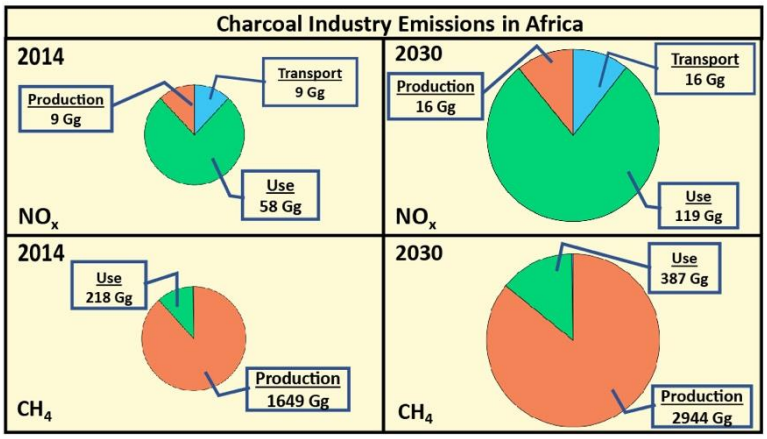

1. THE CHARCOAL SUPPLY CHAIN IN AFRICA

Charcoal is a dominant energy source in Africa and its use is increasing at a rate of 7% a^{-1} due to population growth, urbanization, and low rates of adoption of alternative cleaner sources of energy.[1] More than 80% of urban households in Africa use charcoal,[2] predominantly for cooking. Alternatives like electricity and liquified petroleum gas (LPG) are costly, access to on-grid electricity is limited and notoriously unreliable,[3] and charcoal is more accessible than wood in urban areas as distances to collect fuelwood increase.[4] Charcoal has been identified as a large tropical and global source of the greenhouse gases methane and carbon dioxide (CO_2),[5,6] and a contributor to forest degradation and loss from intensive and unsustainable tree harvesting.[7,8] All steps in the charcoal supply chain also lead to the release of short-lived trace gases and aerosols[9] that are hazardous to health and alter climate.

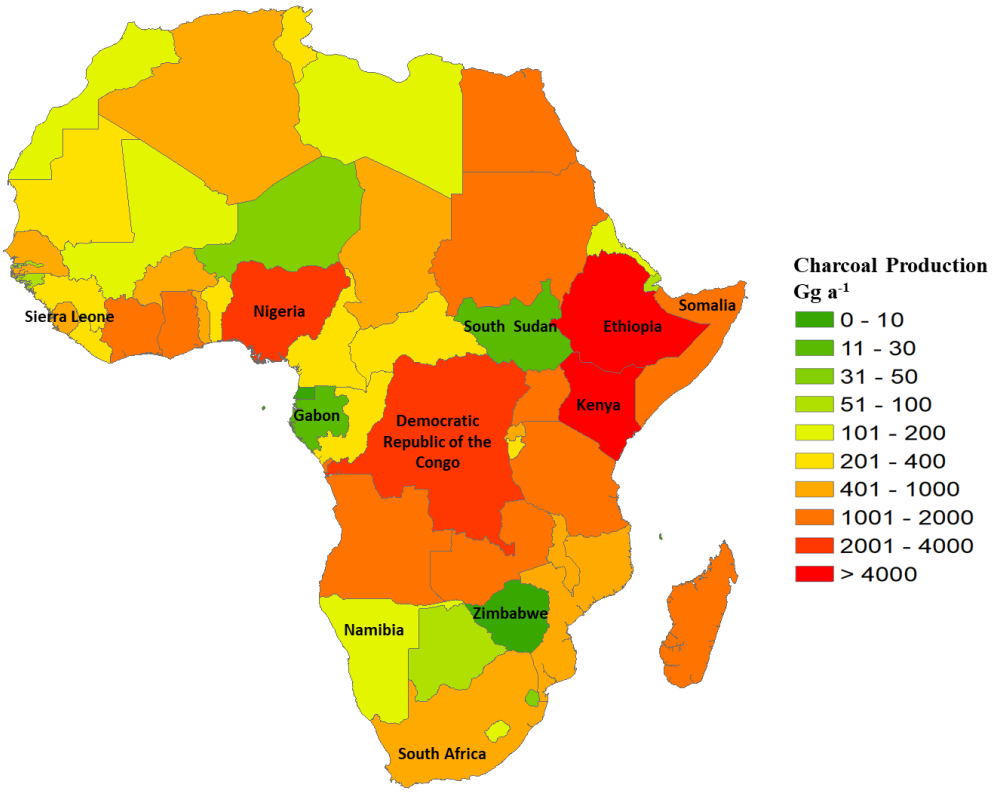

Figure 1. Spatial distribution of charcoal production in Africa in 2014. Data reported for each country is from the United Nations (UN) energy statistics database.[10] Charcoal production is in gigagrams per year (Gg a^{-1}). Total production in 2014 is 41.6 Tg. Countries referred to in the text are labelled.

Africa accounts for > 60% of global charcoal production.[11] We illustrate in Figure 1 that charcoal production, obtained from the UN energy statistics database,[10] occurs across the continent. In 2014, 41.6 Tg of charcoal was produced in Africa,[10] mostly in East Africa (42%) and West Africa (25%). Top producing countries are Ethiopia, Kenya, Nigeria, and the Democratic Republic of the Congo (DRC). Even countries with very low forest cover along the Sahara Desert are significant charcoal producers. According to the same database, almost all (99%) charcoal is used locally, amounting to 41.4 Tg. Of the 1% exported, most is from Somalia (53% of exports) to the Gulf States, and from Namibia (25%) to South Africa or Europe. The charcoal export market in Somalia was estimated at > $250 million for 2013 and

2014, despite a ban imposed in 2012.[12] The few countries with low charcoal production in Figure 1 either have > 90% electricity access (in the case of Gabon) or may not report reliable data. This is likely the case for Zimbabwe (< 10 Gg a^{-1}) and South Sudan (< 30 Gg a^{-1}), as both have low electricity access.[13]

Charcoal combustion produces less smoke than wood,[14] but involves a very inefficient production phase. Most charcoal is produced in rural areas close to main roads and using inefficient earth kilns: piles of wood buried under earth and sod and slow-burned for 2-4 weeks.[15] The finished product is packaged in sacks and loaded onto heavy-duty diesel trucks for transport to cities mainly to be used for residential and commercial cooking.[16] Trace gases and aerosols are emitted throughout the charcoal supply chain[9] and go on to react in the atmosphere to form secondary pollutants (ozone and secondary inorganic or organic aerosols).[17] Ozone and aerosols are hazardous to health (specifically $PM_{2.5}$ or particles with an aerodynamic diameter < 2.5 μm) and offset the Earth's radiative balance.[18,19] The efficiency of conversion of wood to charcoal is very low (9-30 mass %),[20,21] leading to release of products of incomplete combustion: carbon monoxide (CO), methane (CH_4), organic aerosols (OA), and non-methane volatile organic compounds (NMVOCs).[22] Heavy-duty diesel trucks used to transport charcoal to urban centres are outdated, unregulated, and often overloaded, releasing large quantities of black carbon (BC) and nitrogen oxides ($NO_x \equiv NO + NO_2$).[23,24] In urban centres, charcoal used for cooking leads to the release of primary aerosols (BC and OA), NMVOCs and NO_x.[9] In slums, plastic is frequently used to initiate charcoal combustion. When burned, plastic emits hydrochloric acid (HCl)[25] that affects tropospheric budgets of ozone and OH, the dominant oxidant in the atmosphere.[26,27]

Solid fuels have a profound and growing influence on local air quality and health in Africa.[28–30] Ambient concentrations of $PM_{2.5}$ at a charcoal production site in Nigeria, averaged over

phases in the charcoal production process, range from 6,600-34,000 μg m^{-3} during pyrolysis to 100-400 μg m^{-3} during extraction from kilns.[31] Indoor 24-hour mean $PM_{2.5}$ concentrations > 300 μg m^{-3}, sometimes reaching 1500 μg m^{-3}, were measured in homes in Sub-Saharan Africa where charcoal satisfies at least 50% of a household's energy needs.[32] The World Health Organization (WHO) guideline on 24-hour mean $PM_{2.5}$ exposure is 25 μg m^{-3}.[33] Use of existing regional inventories to quantify the air quality and radiative forcing contribution of emissions from the charcoal industry will lead to erroneous results, as these inventories oversimplify the geospatial distribution and temporal variability of charcoal production and use[27,29] and report vehicle usage[27,29] and waste burning[34] emissions in very broad categories.

Here we develop an inventory of directly emitted pollutants and short-lived climate forcers from the charcoal supply chain in Africa for the present-day (2014) and future (2030) to address shortcomings in existing inventories and isolate vehicle usage and waste burning associated with the charcoal industry. We implement the inventory in the GEOS-Chem chemical transport model (CTM) to determine the impact of the charcoal industry across Africa on local surface concentrations of the air pollutants ozone and $PM_{2.5}$ and global tropospheric concentrations and radiative forcing of ozone and aerosols. To put our results in context, we compare these to estimates from anthropogenic sources that are traditionally dominant in Africa. These include open burning of biomass and household use of fuelwood.[29,35]

2. EMISSION INVENTORY DEVELOPMENT

Annual emissions of trace gases (CO, NO, SO_2, NMVOCs and HCl) and primary particles (BC and OA) from charcoal production, use (including plastic burning), and transport are estimated for 2014 in Africa using a standard approach:[36]

$$E_i = A_j \times EF_{i,j} \quad \textbf{(1)}.$$

E_i is annual emissions of pollutant i in grams; A_j is the country-level amount of fuel, j, burned (in kg a^{-1}); and $EF_{i,j}$ is the emission factor of pollutant i in g pollutant per kg fuel j burned. The amount of charcoal produced and used in 2014 is from the UN energy statistics database.[10] The database is curated by the UN Statistics Division using statistics collected with annual questionnaires of contemporary and revised historical data from individual countries.[37]

Most plastic use is in slums on the periphery of cities.[38] There is no activity data on the amount of plastic burned for charcoal use, so we estimate a value for each country as the product of the relative proportion of the urban population living in slums ranging from none in Algeria to >90% in South Sudan in 2014,[39] the quantity of charcoal consumed, and our own speculative guess of the amount of plastic used per kg charcoal consumed (4 g kg^{-1}). We determine 4 g kg^{-1} as the minimum of the ratio of the average mass of a plastic shopping bag (8g)[40] to daily charcoal usage for a 4-person household (2.0-2.6 kg).[41]

We determine diesel use by trucks to transport charcoal to urban centres as the product of the number of trucks required to transport the charcoal, the distance these travel (detailed below), and diesel fuel efficiency (0.25 kg km^{-1}) representative of inefficient and unregulated vehicles.[42] The number of trucks in each country is estimated assuming each truck is heavy duty and transports the recommended maximum payload of 16 tonnes of charcoal. The average distance travelled by the majority of trucks to urban centres is estimated relative to the urban population using scaling factors guided by findings in Philip and Munslow[43] for Maputo in Mozambique. We use a fixed travelling distance from the city centre of 2 km for small cities (≤ 1000 people), a scale factor of 0.025 km per 1000 people to determine the distance travelled to medium-sized cities (1000 < inhabitants ≤ 2 million), and a fixed distance from the city centre of 50 km for large cities (> 2 million people). We obtain urban population by sampling population density from the Gridded Population of the World (GPW) version 4.10 dataset[44]

within the urban extent of the city. The latter we identify as OpenStreetMap residential road networks, a category in the data,[45] with road density ≥ 0.4 miles ha^{-1}.

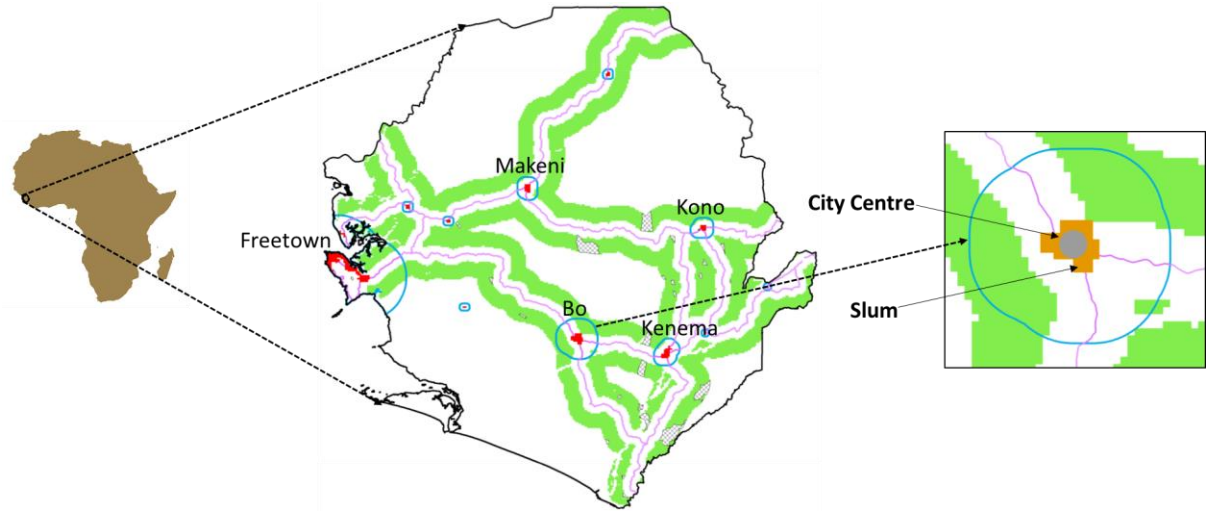

Figure 2. Geospatial mapping of charcoal supply chain activities for Sierra Leone using ArcGIS version 10.4.[46] The centre map shows charcoal production zones (green), urban centres where charcoal is used (red), and major road networks (purple). Blue zones show the extent of roads with the greatest density of trucks transporting charcoal. Hatchings are protected areas (see text for details) that are excluded from charcoal production. The map on the right shows delineation of urban centres into the city centre (grey) and surrounding slums (orange) where plastic is used.

Figure 2 illustrates the approach we take to map charcoal supply chain activities for Sierra Leone in West Africa. In 2014 in Sierra Leone charcoal production and use were equal, each 0.42 Tg. We use OpenStreetMap primary roads,[45] the UN Food and Agriculture Organization (FAO) land cover type,[47] and protected area data[48] to identify viable production zones in each country in Africa. These are typically concentrated 5-15 km from roadways, out of sight but with easy access to transport routes.[49] Viable production zones are those coincident with FAO vegetation types that would be harvested to produce charcoal (forest, woodland, shrubland or

savannah vegetation) (green zones in Figure 2), and not designated as protected areas (hatchings in Figure 2). Plastic burning is mapped to urban populations living 2-15 km from the centre of the city, based on the spatial extent of Kibera, a slum on the periphery of Nairobi, Kenya.[50] This likely overestimates the spatial extent of slums, as Kibera is the largest slum in Africa.[50]

Table 1. Emission factors for charcoal production, use and transport

Activity	Emission Factor [g kg^{-1}] [a]							
	BC	OC	CO	NO	SO_2	CH_4	NMVOCs	HCl
Production [b]	0.02 (0.02)	0.74 (0.72)	255 (52)	0.22 (0.22)	-	39.6 (11.4)	161 (115)	-
Use [b]	1.00	1.30	189 (36)	1.41	-	5.29	5.56	-
Transport	0.14 (0.1)[c]	2.07 (0.2)[c]	23.1 (3)[c]	28.9 (4)[c]	0.35 (0.1)[c]	0.40[d]	2.80[d]	-
Plastic burning [e]	-	-	-	-	-	-	-	77.9

[a] Emission factors (EFs) are in grams of pollutant per kg of fuel consumed. Numbers in parentheses are the estimated variability where this is reported. Dashes denote either no measured or detected EFs. [b] Akagi et al.[9], [c] Zavala et al.[24], [d] Sun et al.[51], [e] Stockwell et al.[25].

Table 1 summarizes the EFs we apply to our gridded data. Values are from Akagi et al.[9] for charcoal production and use. Transport EFs are from measurements for trucks under driving conditions in Mexico City[24] that we assume to be more consistent with conditions in Africa than EFs used to compile European[52] or US[53] regional inventories. Plastic burning is only a significant source of HCl from combustion of chlorinated plastics that, while regulated in Europe and the US, are not in African countries.[54] Values for HCl are from plastic waste burning measurements made during the Nepal Ambient Monitoring and Source Testing Experiment (NAMaSTE) campaign in Nepal.[25]

The conditions under which the EFs in Table 1 are obtained can be highly variable, as indicated by the range in measurements of 100% for BC, OC, and NO from charcoal production. Recent field campaigns in West Africa included measurements of emissions of BC and OC from

charcoal use,[14,23] production,[23] and heavy-duty diesel vehicles (HDDVs).[23] Pfotenhauer et al.[14] also measured CO EFs from charcoal use. Values in Table 1 fall within or close to the range of EFs measured in those studies for charcoal use (BC: <0.15-0.95 g kg^{-1}; OC: 0.48-6.4 g kg^{-1}; CO: 113-276 g kg^{-1}), and OC from HDDVs (1.15-3.93 g kg^{-1}). Whereas, values we use are at least 3-times lower than their OC and BC EFs for charcoal production (OC: 2.92-4.94 g kg^{-1}; BC: 0.06-0.38 g kg^{-1}) and BC EFs from HDDVs (1.15-3.25 g kg^{-1}).

Emissions of pollutants for each activity in each country are calculated as the product of the EFs in Table 1 and fuel use (Eq. (1)). These are then evenly distributed to the charcoal activity locations in each country (Figure 2) and area-weighting is applied to grid these emissions to a uniform 0.1° × 0.1° grid for input to GEOS-Chem.

We determine likely emissions from the charcoal industry in Africa in 2030 by regressing charcoal production for each country against urban population from 2000 to 2014. We find that urban population explains more than 70% of the trends in charcoal production ($R^2 > 0.7$) for countries that collectively account for >80% of charcoal production in 2014. The growth in the charcoal industry ranges from 1.4% a^{-1} for Egypt to 21.1% a^{-1} for Kenya. We obtain a relationship between urban population and charcoal production that varies from -1.3 kg charcoal (urban person)$^{-1}$ a^{-1} for Zimbabwe to 1600 kg charcoal (urban person)$^{-1}$ a^{-1} for Kenya. We apply these to predicted 2030 urban population in each country from the UN[55] to estimate the amount of charcoal produced in 2030 and the relative change in charcoal production (and hence charcoal use and transport) from 2014 to 2030. We apply these relative change values for each country to the gridded 2014 emissions to obtain emissions for 2030. This approach assumes that the relative spatial distribution of emissions in each country is unchanged. In reality, urbanization would increase the spatial extent of charcoal use and unsustainable harvesting of wood leading to forest loss would alter the location of production zones.

The increase in charcoal supply chain activities from 2014 to 2030 in each country ranges from 20% to 130%. Only in Zimbabwe does production and use decrease (by 30%). Total biomass (wood and other dry matter) required to produce charcoal in 2030 is 300-1000 Tg, depending on conversion efficiency. The average past trend in charcoal production across Africa of 7% a^{-1} is sustained to 2030. This results in a doubling in emissions in 2030 relative to 2014 over just 16 years; half the time projected by Bailis et al.[56] for a business-as-usual scenario starting in 2000. Our approach assumes no significant change in EFs, charcoal production and use conversion efficiencies, and the relative proportion of charcoal exported to international markets. One might expect widespread adoption of cleaner alternatives and other initiatives to slow growth in charcoal use. This is not apparent in past behaviour. Imposed bans in countries with intensive charcoal production, such as Somalia and Kenya, have been ineffectual.[57] Historical growth in charcoal production and use has occurred alongside increased adoption of cleaner energy. The use of LPG and electric stoves as primary cooking devices rose by 3.5% a^{-1} (LPG) and 4.3% a^{-1} (electric stoves) from 2000 to 2010.[58] Dominant factors that mitigate much faster adoption of cleaner alternatives to reduce reliance on charcoal include low willingness to pay, low grid connectivity, unreliable electricity supply, and irregular household income.[59] The transition to clean fuels may also be disrupted by the economic recession anticipated as a result of the COVID-19 pandemic.[60,61]

3. INCORPORATION OF THE INVENTORY IN GEOS-CHEM

We use GEOS-Chem version 12.0.0 (https://zenodo.org/record/1343547) coupled to the rapid radiative transfer model (RRTMG)[62] to determine the contribution of the charcoal supply chain in Africa to local surface concentrations of ozone and $PM_{2.5}$ and to regional and global direct radiative effects of aerosols and ozone from the difference in these modelled parameters with and without our inventory. GEOS-Chem is simulated at a horizontal resolution of 2° × 2.5°

(latitude × longitude) and is driven with NASA Global Modeling and Assimilation Office (GMAO) Modern-Era Retrospective Analysis version 2 (MERRA-2) reanalysis meteorology.

We partition emission factors for total NMVOCs (Table 1) into individual components based on source profiles from Akagi et al.[9] for charcoal production and use and from Zavala et al.[24] for trucks. We also derive representative seasonal scaling factors for charcoal production and transport, and diurnal scaling factors for charcoal use. Kambewa et al.[63] report from field observations that most charcoal is produced in the rainy season, as charcoal producers capitalise on higher charcoal prices in this season when other fuel sources are unreliable. We assume that 60% of charcoal is produced and transported in the wet season compared to 40% in the transition and dry seasons. The timing and length of charcoal production in the wet season varies spatially to represent spatial variability in these across the continent. The diurnal scaling we use assumes that most charcoal, primarily for cooking, is used from 06h00 to 20h00 local time. The other emission sources in GEOS-Chem relevant to Africa are from the Global Fire Emissions Database version 4 (GFED4)[64] for open fires, Diffuse and Inefficient Combustion Emissions in Africa (DICE-Africa)[29] for anthropogenic inefficient combustion excluding charcoal production and use, and Community Emissions Data System (CEDS)[65] for industry, power generation and open burning of trash. The model also includes natural emissions of biogenic NMVOCs,[66] soil NO_x,[67] and dust.[68] Emissions are regridded to the GEOS-Chem grid and seasonal and diurnal scaling factors are applied with the Harvard-NASA Emissions Component (HEMCO) emissions processing package.[69]

GEOS-Chem includes detailed gas- and aerosol-phase chemistry and loss processes (wet and dry deposition) to represent formation and loss of ozone and relevant individual components of $PM_{2.5}$: sulfate, nitrate, ammonium,[70,71] OA,[72] and BC.[73] GEOS-Chem representation of $PM_{2.5}$ in Africa has already been evaluated with a similar configuration of the model to that

used here. In that study, modelled $PM_{2.5}$ reproduced annual mean $PM_{2.5}$ measured at limited surface network sites in South Africa and derived with global satellite observations of aerosol optical depth (AOD).[74] RRTMG calculates instantaneous long- and short-wave fluxes.[62] We sample top-of-the-atmosphere all-sky fluxes associated with aerosols in the shortwave only and associated with ozone in the short- and long-wave. Additional details of model treatment of aerosols and calculation of $PM_{2.5}$ are in the supporting information. Meteorology for 2014 is used for both model simulations that use the 2014 and 2030 inventory to isolate the effects of emissions only. We sample the model in 2014 following two months of spin-up for chemical initialization.

4. PRESENT-DAY CHARCOAL INDUSTRY EMISSIONS

The amount of wood pyrolysed to produce charcoal in 2014, assuming a conversion efficiency of 9-30%,[20,21] is 140-460 Tg. This represents 6-22% of annual open fire dry matter burned from the GFEDv4.1 biomass burning inventory for Africa.[75] Based on the emission estimates of our study, the importance of charcoal relative to open fires may be increasing rapidly. In West Africa, for example, we estimate that 35-120 Tg fuelwood was used to produce charcoal in 2014. This is 2-6 times the 21 Tg obtained by Lacaux et al.[76] for West Africa in 1992 for a conversion efficiency of 28%. The amount of charcoal produced (Figure 1) and used in 2014 is 1.4 times more than that in the regional DICE-Africa inventory for 2013 (29.8 Tg from production; 27.7 Tg from use),[29] even though DICE-Africa activity data is from the same database and most charcoal production and EFs for DICE-Africa are similar to those used here (Table S1). Larger production and use in our inventory is due to a combination of annual growth from 2013 to 2014, availability of data for more countries (47 countries) than was available for DICE-Africa (43), and a 32% increase in the revised UN database charcoal production and use statistics used in this study. The latter we estimate by comparing data for the same countries for 2013 used in DICE-Africa and the UN data we use. Fuel usage for

transporting charcoal of 0.07 Tg represents just 0.2% of all motor gasoline used for transport in Africa in 2014.[10]

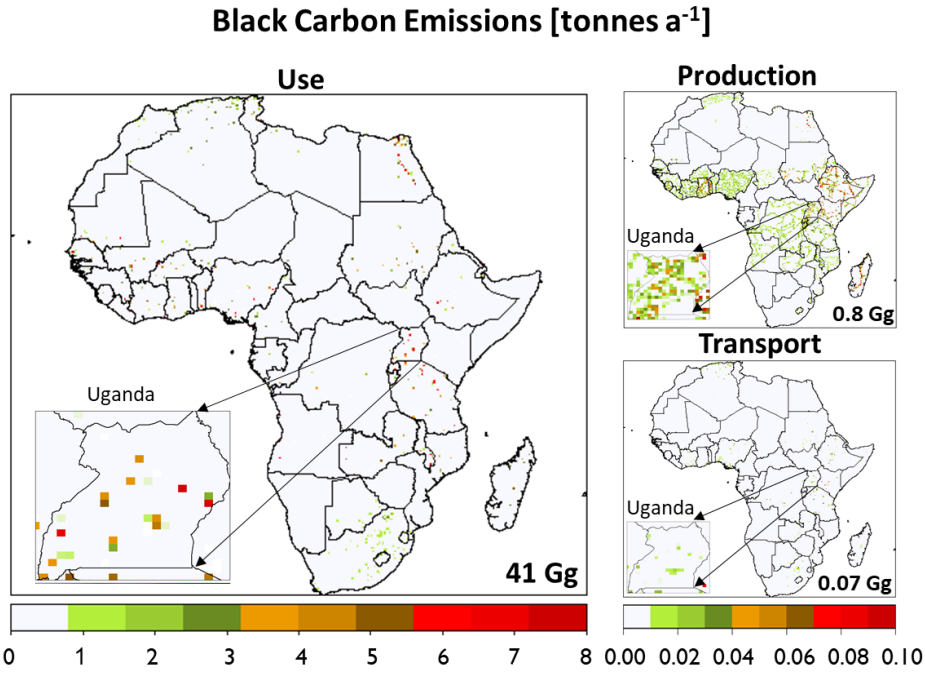

Figure 3. Spatial distribution of BC emissions from charcoal use (left), production (top right), and transport (bottom right) in Africa in 2014 at 0.1° × 0.1°. Inset images illustrate the spatial distribution of BC emissions for Uganda. Inset values are emission totals for the continent in 2014.

Figure 3 shows the spatial distribution of BC emissions from charcoal production, use and transport in Africa in 2014. We use BC to illustrate the spatial distribution of emissions, since we find that all other pollutants show similar spatial distribution, apart from HCl (emitted in slums only) and SO_2 (from transport only). Emissions from all activities peak in East and West Africa (as is expected from Figure 1). Intense production in rural areas is concentrated along major roadways, and consumption and transport peak in urban centres where people and truck traffic are concentrated (Figure 2).

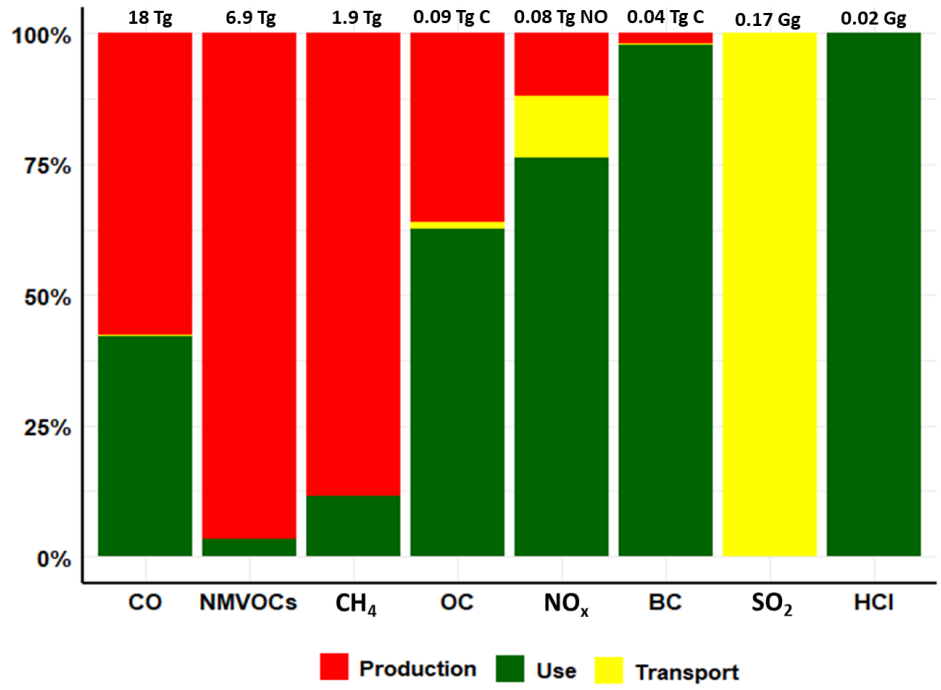

Figure 4. Contribution of charcoal activities to emitted pollutants in 2014. Total emissions are given for each pollutant. Colours distinguish emissions for charcoal production (red), use (green), and transport (yellow).

Figure 4 shows total emissions of each pollutant and the relative contribution of the different activities to the total in 2014. Emissions from charcoal production are dominated by CO (57.7% of total CO emissions), NMVOCs (96.6%), and CH_4 (88.3%) and reflect incomplete combustion under low-oxygen conditions. The majority of NO_x and BC emissions are from use in urban centres (76.1% for NO_x; 97.8% for BC), due to higher conversion efficiencies compared to charcoal production. The NMVOC-to-NO_x emission ratios are much higher for production (700:1) than use (4:1). This indicates much greater sensitivity of ozone production to NO_x emissions in charcoal production zones than in urban areas,[66] though this effect will be diluted at the coarse resolution of the model used here.

Charcoal production should make a larger contribution to OC emissions than its use, as charcoal production is a very inefficient combustion process, but we obtain the opposite in our inventory: 36.1% from production; 62.7% from use. The BC and OC EFs that we use from

Akagi et al.[9] are originally from Bond et al.[79], with reported uncertainties of 110% for BC and 91% for OC. The mean of the OC EFs for charcoal production from the recent field measurements obtained by Keita et al.[23] of 3.93 g kg^{-1} is 5-times higher than 0.74 g kg^{-1} used in this work (Table 1). If instead we used the Keita et al.[23] EFs, the relative contribution of OC would be 69.2% production, 30.4% use. Similarly, at least 10-times higher BC EFs from Keita et al.[23] for HDDV would increase the contribution of trucks to total BC emissions to 17% compared to only 2% in Figure 4 and increase total BC emissions from 40 to 50 Gg.

In cities, emissions are higher in slums than the city centre, reflecting greater population density and dependence on charcoal for energy generation in slums. HCl is exclusively from plastic burning in our inventory. There are also HCl emissions from burning fuelwood, but these are much lower than from burning plastic.[25] The total plastic burned in 2014 to initiate combustion, obtained as the product of the rate of usage (4 g kg^{-1}) and the mass of charcoal used in slums (Figure 2), is 260 tonnes. Values for individual countries are in Figure S1. Plastic burning also releases OA, BC and CO. Total emissions of these from burning 260 tonnes of plastic is 2.2 tonnes BC, 8.8 tonnes OC, and 22 tonnes CO using reported EFs of BC[80], OC[80] and CO[25]. These are at least 3 orders of magnitude less than charcoal industry emission totals (Figure 4). All the SO_2 is from transport, as there are no detectable emissions of SO_2 from charcoal production and use.[9,81] With the exception of NO_x and SO_2 emissions, transport contributes <2% to total emissions. A similar small contribution (0.15%) of transport to emissions of CO_2 from the charcoal supply chain was estimated by Ekeh et al.[82] for Kampala, the capital city of Uganda.

Emissions from this work are higher than those in DICE-Africa[29] for charcoal use due to differences in activity factors already discussed, but much lower than DICE-Africa for charcoal production. That inventory used the same Akagi et al.[9] charcoal production EFs as in Table 1,

but applied these as per kg fuelwood required to produce charcoal rather than per kg charcoal produced. They used a conversion efficiency of 20% to estimate the mass of fuelwood required from the reported mass of charcoal produced, leading to a 5-fold overestimate in emissions in that inventory. After we correct for this error in the DICE-Africa charcoal production emissions, we find that the BC, OC, CO, NMVOCs and CH_4 emissions from this work are higher than DICE-Africa charcoal production and use emissions by 30-80%. This is due to differences in activities already discussed. Table S2 compares individual species emissions from DICE-Africa and our inventory.

Uncertainties in our emission inventory result from limited availability of activity data, our assumptions about activities in the absence of data (specifically trucks and plastic burning), limited information about EFs representative of conditions in Africa, and extrapolation of information from a few reports or local case studies to the whole continent. Even so, emissions estimates from our inventory suggest that the charcoal industry makes a substantial contribution to biomass emissions in Africa. Our estimate of CH_4 emissions from the charcoal supply chain, mostly from production (Figure 3), is 40% of CH_4 emissions from open fires in Africa from the global GFEDv4.1 inventory in 2014.[75] Rapid urbanisation is driving an increase in charcoal production of ~7% a^{-1} across Africa. Burned area from open fires in countries in West Africa decreased by 0.7-2.0% a^{-1} from 2001 to 2012 due to cropland expansion alone.[83] At these rates, CH_4 from the charcoal industry in West Africa may surpass that from open fires by 2025.

5. AIR POLLUTION AND CLIMATE FORCING OF CHARCOAL EMISSIONS

The top panel of Figure 5 shows GEOS-Chem annual mean surface concentrations of $PM_{2.5}$ and ozone for 2014 from all sources. $PM_{2.5}$ is mostly from windblown Sahara Desert dust. Surface ozone in North Africa is influenced by emissions in Europe[84] and those in southern

Africa by emissions from industry and power generation in South Africa, exacerbated by large-scale recirculation of pollution-laden air.[85,86] The bottom panel of Figure 5 shows the enhancement in annual mean surface $PM_{2.5}$ and ozone in 2014 due to the charcoal supply chain, obtained as the difference in GEOS-Chem simulations with and without our inventory. These are likely conservative, as we use OC EFs for charcoal production and BC EFs for HDDV that are much lower than recent field measurements[23]. The effect of using these would be greatest in rural areas, due to an increase in mass concentrations of OA along production zones. Charcoal industry $PM_{2.5}$ is highest in East and West Africa and closely follows supply chain emissions (Figure 3). The peak enhancement of 1.3 μg m^{-3} occurs at the border between Kenya and Uganda and propagates up to ~2 km altitude in the model. In southern and East Africa annual mean $PM_{2.5}$ is <40 μg m^{-3}, so a unit change in $PM_{2.5}$ would increase the risk of premature mortality by 0.8%, according to the relationship between $PM_{2.5}$ and premature mortality from the meta-regression analysis of Vodonos et al.[74,87] That relationship was derived without cohorts from African countries. A weaker health response would be expected for North and West Africa where annual mean $PM_{2.5}$ far exceeds 40 μg m^{-3}.[74,87] Surface ozone enhancements due to the charcoal supply chain are small, peaking at just 0.7 ppbv coincident with the densely populated cities Nairobi and Kampala in East Africa. The contribution of open fire emissions to surface ozone in Africa is much larger (10-50 ppbv).[35] The enhancement we estimate for 2030 is on average a factor of 1.4 more for $PM_{2.5}$ and 1.8 more for ozone than is obtained in 2014.

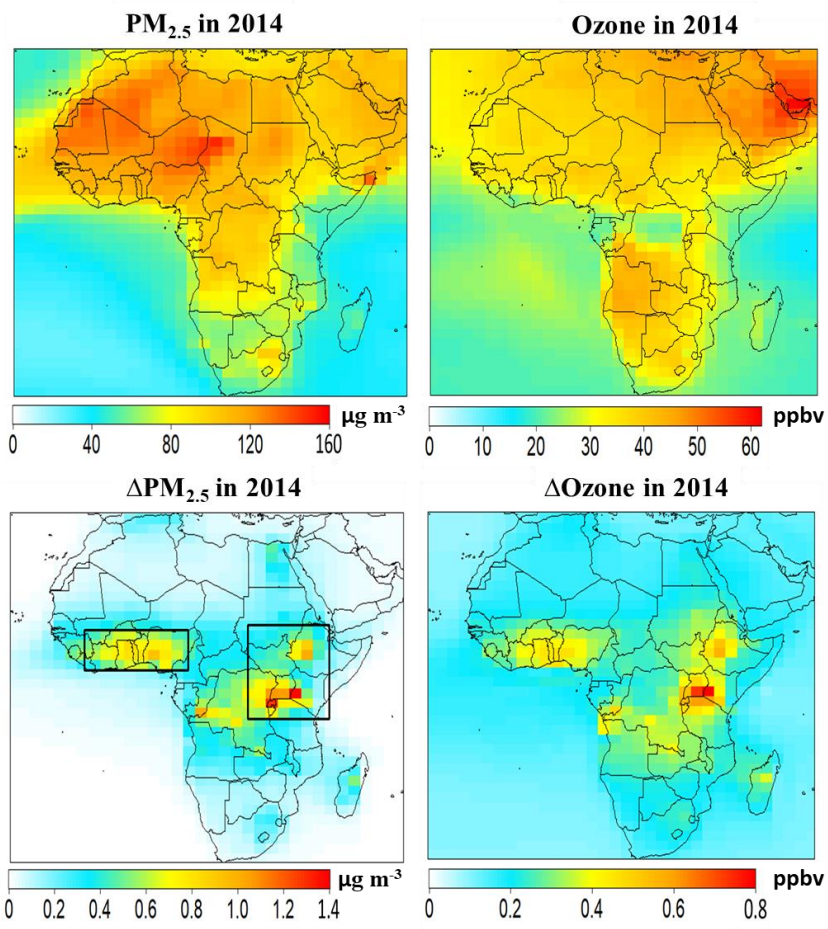

Figure 5. The effect of the charcoal supply chain on surface $PM_{2.5}$ and ozone in 2014. Panels show the spatial distribution of GEOS-Chem annual mean surface $PM_{2.5}$ (left) and ozone (right) from all sources (top) and from the charcoal supply chain only (bottom) (see text for details). Black boxes show domains used to generate Figure 6.

Figure 6 shows the seasonality of the enhancement in surface $PM_{2.5}$ and ozone from charcoal where these pollutants peak in East and West Africa (Figure 5). $PM_{2.5}$ seasonality is stronger in West than East Africa and is opposite to the seasonality that we impose for charcoal production emissions (60% in the wet season). This is because of efficient dispersal of air pollution by the south-westerlies of the West African Monsoon in June-August. Spatial displacement of $PM_{2.5}$ to the northeast in the wet season in West Africa supports this (not shown). In December-February, $PM_{2.5}$ accumulates in West Africa due to very stagnant

conditions resulting from a natural inversion across West Africa established by southerly shift of the warm Harmattan winds.[88] Ozone seasonality is also stronger in West than East Africa and is enhanced in all months except the dry season. The dry season includes emissions of NO_x from intense and widespread biomass burning, whereas outside the biomass burning season NO_x emissions are relatively low. This leads to sensitivity of ozone formation to NO_x in West Africa outside the dry season[89] and the seasonal pattern shown in Figure 6. Most charcoal NO_x emissions come from charcoal use (Figure 4) that has diurnal variability, but no seasonality in the model.

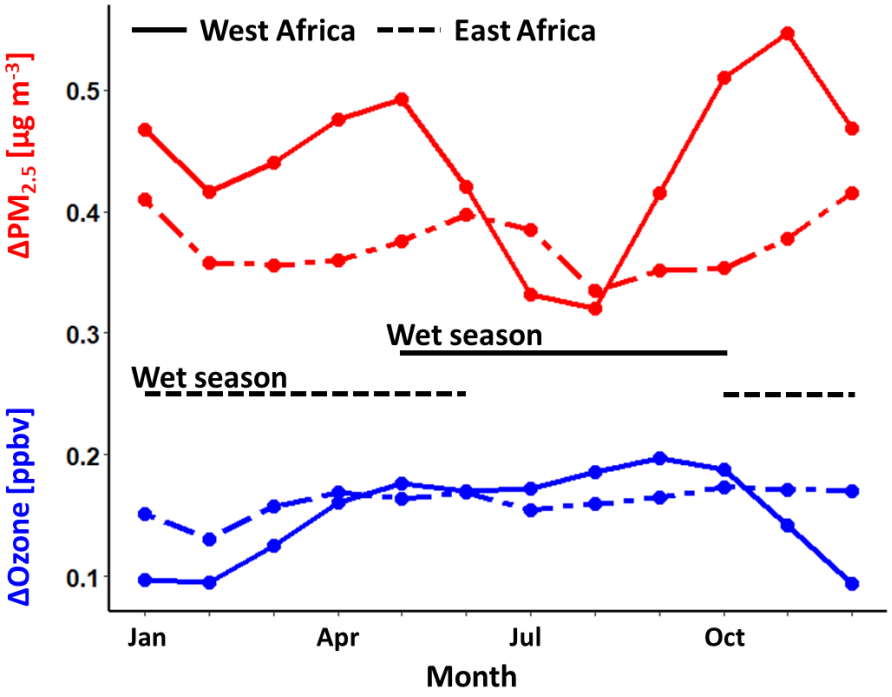

Figure 6. Seasonality of surface $PM_{2.5}$ and ozone from charcoal emissions in Africa in 2014. Points are monthly means obtained as the difference in GEOS-Chem $PM_{2.5}$ (red) and ozone (blue) with and without our inventory over West Africa (solid line) and East Africa (dashed line). Domains sampled are indicated in Figure 5. Black lines show the duration of the wet and transition seasons for West Africa (solid line) and East Africa (dashed line).

Figure 7 shows 2014 all-sky top-of-the-atmosphere (TOA) direct radiative forcing due to aerosols and ozone from the charcoal supply chain in Africa. These are obtained as the difference in GEOS-Chem-RRTMG calculated atmospheric fluxes with and without our inventory. The all-sky TOA direct aerosol forcing is localised over the continent close to large urban sources and is negative, mostly due to negative OA radiative forcing. The positive contribution from BC is small, peaking at just 3 mW m^{-2}. The average aerosol radiative forcing for the continent and a portion of the Middle East (25.4°W-57.8°E and 34.8°S-37.3°N) is -30 mW m^{-2}; much more than the response of -4.1 mW m^{-2} from a 10% reduction in early 1990s open fire emissions for a similar domain and using a CTM and an offline radiative transfer model.[90] The 10% emissions reduction in that study is similar in magnitude to our CO and NMVOCs emissions for 2014, but is more than our BC, OC, and NO_x.

The all-sky TOA direct ozone radiative forcing extends across the tropics and subtropics and is mostly positive. There are some locations with negative forcing in East Africa. These occur over cities in Kenya (Nairobi), Uganda (Kampala), and Ethiopia (Addis Ababa) that have large enhancements in $PM_{2.5}$ from charcoal emissions (Figure 5). The negative ozone forcing results from reduced availability of light due to absorption by strong absorbers like BC emitted during urban charcoal use (Figures 4-5). Positive ozone radiative forcing peaks at 4.2 mW m^{-2} over the mid-Atlantic in 2014 and the average for the south and mid-Atlantic Ocean (box in Figure 7) is 2.2 mW m^{-2}. The ozone radiative forcing estimated for Africa in the 10% open fires emissions reduction study[90] is -4.6 mW m^{-2}; more than double the magnitude of the response we obtain of +1.9 mW m^{-2} in 2014.

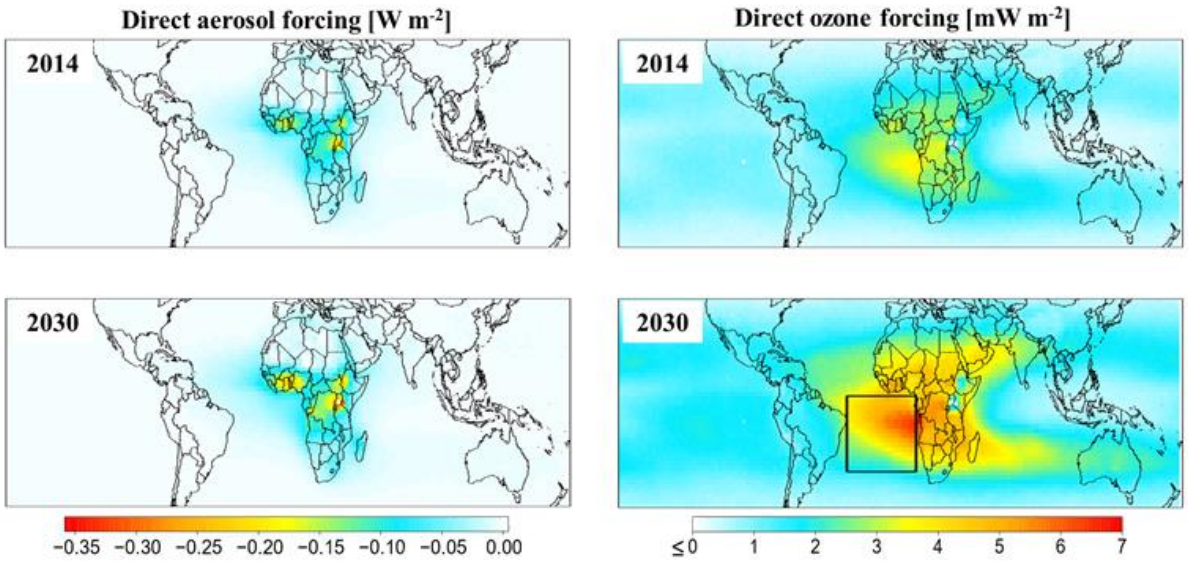

Figure 7. Direct radiative forcing in the tropics and subtropics due to the charcoal supply chain in Africa now and in the future. Simulated annual mean all-sky top-of-the-atmosphere direct aerosol shortwave (left) and ozone longwave and shortwave (right) forcing for 2014 (top) and 2030 (bottom) from GEOS-Chem coupled to RRTMG (see text for details). The black box is the mid-Atlantic Ocean region discussed in the text.

Figure 8 shows the vertical distribution of modelled ozone for 2014 north and south of the Equator. Charcoal industry emissions increase ozone at the surface (Figure 5) and throughout the troposphere (Figure 8), as ozone precursor emissions of NO_x, NMVOCs, CO, and CH_4 far exceed ozone destruction emissions of HCl (Figure 4). The ozone enhancements associated with the positive TOA direct ozone radiative forcing in Figure 7 occur aloft and predominantly in the upper troposphere (above 350 hPa; > 8 km). This is associated with peak ozone radiative forcing efficiency aloft in the tropics[91] and an increase in ozone production efficiency (ozone produced per molecule of NO_x lost to temporary reservoirs or permanent sinks) with altitude.[92,93]

Figure 7 also includes future (2030) annual mean all-sky TOA direct aerosol and ozone radiative forcing from the charcoal supply chain in Africa. The mean all-sky TOA aerosol direct forcing for Africa is -40 mW m^{-2}; 1.3 times the aerosol direct forcing in 2014. The peak all-sky TOA ozone direct radiative forcing is 6.3 mW m^{-2} over the Atlantic Ocean region (box in Figure 7). The mean for Sub-Saharan Africa (30°W-60°E, 40°S-10°N) almost doubles from 1.9 mW m^{-2} in 2014 to 3.4 mW m^{-2} in 2030 and can be compared to 10 mW m^{-2} and 15 mW m^{-2} direct ozone radiative forcing estimated for all household biofuel use and open burning of biomass, respectively, in Sub-Saharan Africa for 2030 relative to 1995 obtained using a general circulation model with a middle-of-the-road future scenario to calculate 2030 emissions.[94]

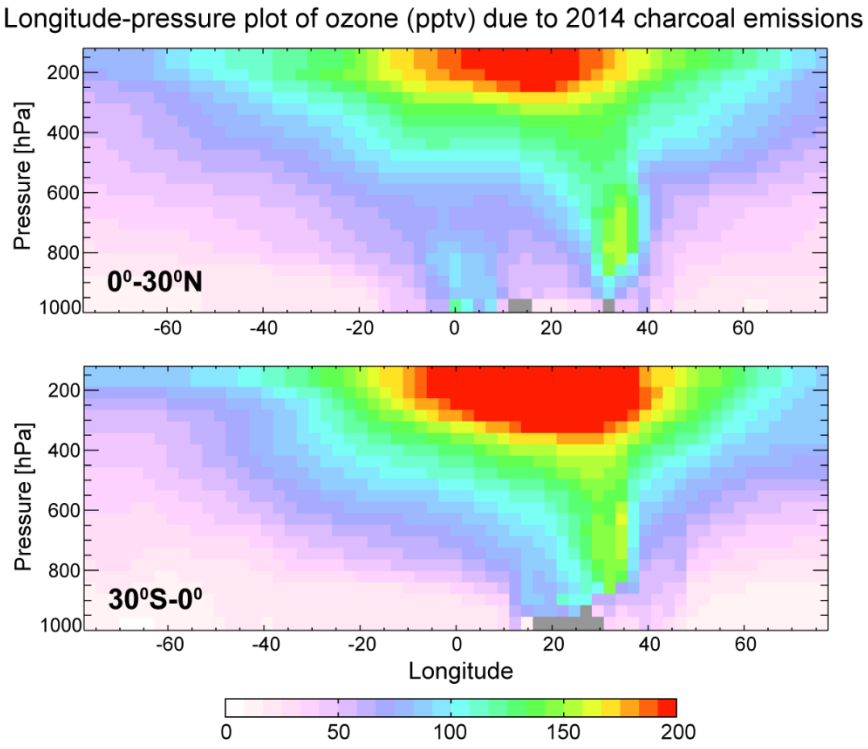

Figure 8. Vertical distribution of tropospheric ozone attributed to the charcoal supply chain in Africa in 2014. Longitude-pressure plot of GEOS-Chem ozone enhancements in the northern (top) and southern (bottom) hemispheres averaged into 50 hPa bins. Tropopause height is from MERRA-2 meteorology.

The health study by Marais et al.[74] provides support for widespread adoption of renewable energy in Africa by calculating a large health burden due to exposure to ambient $PM_{2.5}$ from future fossil fuel use for transport and energy production. Our work further incentivizes the need for this energy transition by showing that the charcoal industry in Africa has a large and rapidly increasing influence on local air pollution and local and regional climate. Africa is urbanizing faster than anywhere else in the world, driving growth in the charcoal industry. Estimates of the influence of the charcoal industry on air quality and climate are particularly sensitive to the choice of emission factors, so there is critical need for ongoing research to measure emission factors representative of a range of production practices (kilns, conversion efficiencies, emission mitigation measures) and usage conditions (cookstoves, charcoal quality). Also in need are extensive geospatial information of charcoal kilns aided by remote sensing and machine learning[95], continuous measurements of atmospheric composition to evaluate air quality and climate models in priority regions identified in this work (East and West Africa), estimates of health risks of exposure to charcoal pollution at production sites and indoors, and incorporation of air pollutants and short-lived climate forcers in environmental sustainability assessments of this widely adopted energy source.

AUTHOR INFORMATION

Corresponding Author

*Email: e.marais@ucl.ac.uk

Author Contributions

ASB developed the emission inventory, conducted the GEOS-Chem simulations, analysed and interpreted the data, and prepared the manuscript. EAM provided supervisory guidance, contributed to data analysis, and assisted in the writing, with co-supervision from ARM.

Notes

The authors declare no competing financial interest. Gridded emission inventory data and GEOS-Chem model output are available at https://github.com/asbock2/PhD-Research

ACKNOWLEDGEMENTS

This work was funded by a PhD research scholarship from the Islamic Development Bank Group awarded to ASB, and a NERC/EPSRC grant (EP/R513465/1) awarded to EAM. The authors are grateful to Dr Loretta Mickley for helpful discussions on ozone radiative forcing.

Supporting Information.

The supporting document includes a description of the representation of aerosols in GEOS-Chem and calculation of $PM_{2.5}$, as well as the spatial distribution of the amount of plastic burned (Figure S1), and comparison of emission factors (Table S1) and emissions (Table S2) of air pollution precursors from this and previous work.

REFERENCES

(1) Arnold, J. E. M.; Köhlin, G.; Persson, R. Woodfuels, Livelihoods, and Policy Interventions: Changing Perspectives. *World Dev.* **2006**, *34* (3), 596–611. https://doi.org/10.1016/j.worlddev.2005.08.008.

(2) Zulu, L. C.; Richardson, R. B. Charcoal, Livelihoods, and Poverty Reduction: Evidence from Sub-Saharan Africa. *Energy Sustain. Dev.* **2013**, *17* (2), 127–137. https://doi.org/10.1016/J.ESD.2012.07.007.

(3) Sawe, E. N. Sustainable Charcoal and Firewood Production and Use in Africa. In *Bioenergy for sustainable development in Africa*; 2014; Vol. 9789400721, pp 75–80. https://doi.org/10.1007/978-94-007-2181-4-7.

(4) Akpalu, W.; Dasmani, I.; Aglobitse, P. B. Demand for Cooking Fuels in a Developing Country: To What Extent Do Taste and Preferences Matter? *Energy Policy* **2011**, *39* (10), 6525–6531. https://doi.org/10.1016/J.ENPOL.2011.07.054.

(5) Chidumayo, E. N.; Gumbo, D. J. The Environmental Impacts of Charcoal Production in Tropical Ecosystems of the World: A Synthesis. *Energy Sustain. Dev.* **2013**, *17* (2), 86–94. https://doi.org/https://doi.org/10.1016/j.esd.2012.07.004.

(6) Bailis, R.; Drigo, R.; Ghilardi, A.; Masera, O. The Carbon Footprint of Traditional Woodfuels. *Nat. Clim. Chang.* **2015**, *5*, 266.

(7) Mwampamba, T. H. Has the Woodfuel Crisis Returned? Urban Charcoal Consumption in Tanzania and Its Implications to Present and Future Forest Availability. *Energy Policy* **2007**, *35* (8), 4221–4234. https://doi.org/https://doi.org/10.1016/j.enpol.2007.02.010.

(8) Sedano, F.; Lisboa, S. N.; Duncanson, L.; Ribeiro, N.; Sitoe, A.; Sahajpal, R.; Hurtt, G.; Tucker, C. J. Monitoring Forest Degradation from Charcoal Production with Historical Landsat Imagery. A Case Study in Southern Mozambique. *Environ. Res. Lett.* **2020**, *15* (1), 015001. https://doi.org/10.1088/1748-9326/ab3186.

(9) Akagi, S. K.; Yokelson, R. J.; Wiedinmyer, C.; Alvarado, M. J.; Reid, J. S.; Karl, T.; Crounse, J. D.; Wennberg, P. O. Emission Factors for Open and Domestic Biomass Burning for Use in Atmospheric Models. *Atmos. Chem. Phys.* **2011**, *11* (9), 4039–4072. https://doi.org/10.5194/acp-11-4039-2011.

(10) UN. Energy Statistics Database | United Nations Statistics Division http://data.un.org/Data.aspx?d=EDATA&f=cmID%3ACH#EDATA (accessed Aug 15, 2017).

(11) FAO. FAOSTAT (dataset) http://faostat3.fao.org/%0Afaostat-

gateway/go/to/browse/F/FO/E (accessed Jun 20, 2018).

(12) Michelle, N.; Charbonneau, L. Exclusive: Illegal Somali charcoal exports fuel Islamist rebels, warlords https://www.reuters.com/article/us-somalia-charcoal-un/exclusive-illegal-somali-charcoal-exports-fuel-islamist-rebels-warlords-idUSKCN0HZ2E120141010 (accessed May 5, 2019).

(13) World Bank. Access to electricity (% of population) https://data.worldbank.org/indicator/EG.ELC.ACCS.ZS (accessed Feb 2, 2018).

(14) Pfotenhauer, D. J.; Coffey, E. R.; Piedrahita, R.; Agao, D.; Alirigia, R.; Muvandimwe, D.; Lacey, F.; Wiedinmyer, C.; Dickinson, K. L.; Dalaba, M.; Kanyomse, E.; Oduro, A.; Hannigan, M. P. Updated Emission Factors from Diffuse Combustion Sources in Sub-Saharan Africa and Their Effect on Regional Emission Estimates. *Environ. Sci. Technol.* **2019**, *53*, 6392–6401. https://doi.org/10.1021/acs.est.8b06155.

(15) Demirbas, A. Sustainable Charcoal Production and Charcoal Briquetting. *Energy Sources, Part A Recover. Util. Environ. Eff.* **2009**, *31* (19), 1694–1699. https://doi.org/10.1080/15567030802094060.

(16) Malimbwi, R. E.; Zahabu, E. M. *Woodlands and the Charcoal Trade: The Case of Dar Es Salaam City*; Working Papers of the Finnish Forest Research Institute; 98–114; Tanzania, 2008.

(17) Crutzen, P. J.; Andreae, M. O. Biomass Burning in the Tropics: Impact on Atmospheric Chemistry and Biogeochemical Cycles. *Science (80-.).* **1990**, *250* (4988), 1669–1678. https://doi.org/10.1126/science.250.4988.1669.

(18) Von Schneidemesser, E.; Monks, P. S.; Allan, J. D.; Bruhwiler, L.; Forster, P.; Fowler, D.; Lauer, A.; Morgan, W. T.; Paasonen, P.; Righi, M.; Sindelarova, K.; Sutton, M. A. Chemistry and the Linkages between Air Quality and Climate Change. *Chem. Rev.*

2015, *115* (10), 3856–3897. https://doi.org/10.1021/acs.chemrev.5b00089.

(19) Burnett, R.; Chen, H.; Szyszkowicz, M.; Fann, N.; Hubbell, B.; Pope, C. A.; Apte, J. S.; Brauer, M.; Cohen, A.; Weichenthal, S.; Coggins, J.; Di, Q.; Brunekreef, B.; Frostad, J.; Lim, S. S.; Kan, H.; Walker, K. D.; Thurston, G. D.; Hayes, R. B.; Lim, C. C.; Turner, M. C.; Jerrett, M.; Krewski, D.; Gapstur, S. M.; Diver, W. R.; Ostro, B.; Goldberg, D.; Crouse, D. L.; Martin, R. V.; Peters, P.; Pinault, L.; Tjepkema, M.; Donkelaar, A. van; Villeneuve, P. J.; Miller, A. B.; Yin, P.; Zhou, M.; Wang, L.; Janssen, N. A. H.; Marra, M.; Atkinson, R. W.; Tsang, H.; Thach, T. Q.; Cannon, J. B.; Allen, R. T.; Hart, J. E.; Laden, F.; Cesaroni, G.; Forastiere, F.; Weinmayr, G.; Jaensch, A.; Nagel, G.; Concin, H.; Spadaro, J. V. Global Estimates of Mortality Associated with Long-Term Exposure to Outdoor Fine Particulate Matter. *Proc. Natl. Acad. Sci.* **2018**, *115* (38), 9592–9597. https://doi.org/10.1073/PNAS.1803222115.

(20) FAO. *The Charcoal Transition: Greening the Charcoal Value Chain to Mitigate Climate Change and Improve Local Livelihoods*; Rome, 2017.

(21) Yevich, R.; Logan, J. A. An Assessment of Biofuel Use and Burning of Agricultural Waste in the Developing World. *Global Biogeochem. Cycles* **2003**, *17*, 1095. https://doi.org/10.1029/2002gb001952.

(22) Yokelson, R. J.; Griffith, D. W. T.; Ward, D. E. Open-Path Fourier Transform Infrared Studies of Large-Scale Laboratory Biomass Fires. *J. Geophys. Res. Atmos.* **1996**, *101* (D15), 21067–21080. https://doi.org/10.1029/96jd01800.

(23) Keita, S.; Liousse, C.; Yoboué, V.; Dominutti, P.; Guinot, B.; Assamoi, E. M.; Borbon, A.; Haslett, S. L.; Bouvier, L.; Colomb, A.; Coe, H.; Akpo, A.; Adon, J.; Bahino, J.; Doumbia, M.; Djossou, J.; Galy-Lacaux, C.; Gardrat, E.; Gnamien, S.; Léon, J. F.; Ossohou, M.; Touré N'Datchoh, E.; Roblou, L. Particle and VOC Emission Factor

Measurements for Anthropogenic Sources in West Africa. *Atmos. Chem. Phys.* **2018**, *18* (10), 7691–7708. https://doi.org/10.5194/acp-18-7691-2018.

(24) Zavala, M.; Molina, L. T.; Yacovitch, T. I.; Fortner, E. C.; Roscioli, J. R.; Floerchinger, C.; Herndon, S. C.; Kolb, C. E.; Knighton, W. B.; Hugo Paramo, V.; Zirath, S.; Mejía, J. A.; Jazcilevich, A. Emission Factors of Black Carbon and Co-Pollutants from Diesel Vehicles in Mexico City. *Atmos. Chem. Phys.* **2017**, *17* (24), 15293–15305. https://doi.org/10.5194/acp-17-15293-2017.

(25) Stockwell, C. E.; Christian, T. J.; Goetz, J. D.; Jayarathne, T.; Bhave, P. V.; Praveen, P. S.; Adhikari, S.; Maharjan, R.; DeCarlo, P. F.; Stone, E. A.; Saikawa, E.; Blake, D. R.; Simpson, I. J.; Yokelson, R. J.; Panday, A. K. Nepal Ambient Monitoring and Source Testing Experiment (NAMaSTE): Emissions of Trace Gases and Light-Absorbing Carbon from Wood and Dung Cooking Fires, Garbage and Crop Residue Burning, Brick Kilns, and Other Sources. *Atmos. Chem. Phys.* **2016**, *16* (17), 11043–11081. https://doi.org/10.5194/acp-16-11043-2016.

(26) Wang, X.; Jacob, D. J.; Eastham, S. D.; Sulprizio, M. P.; Zhu, L.; Chen, Q.; Alexander, B.; Sherwen, T.; Evans, M. J.; Lee, B. H.; Haskins, J. D.; Lopez-Hilfiker, F. D.; Thornton, J. A.; Huey, G. L.; Liao, H. The Role of Chlorine in Global Tropospheric Chemistry. *Atmos. Chem. Phys.* **2019**, *19* (6), 3981–4003. https://doi.org/10.5194/acp-19-3981-2019.

(27) Sherwen, T.; Evans, M. J.; Carpenter, L. J.; Schmidt, J. A.; Mickley, L. J. Halogen Chemistry Reduces Tropospheric O_3 Radiative Forcing. *Atmos. Chem. Phys.* **2017**, *17*, 1557–1569. https://doi.org/10.5194/acp-17-1557-2017.

(28) Liousse, C.; Assamoi, E.; Criqui, P.; Granier, C.; Rosset, R. Explosive Growth in African Combustion Emissions from 2005 to 2030. *Environ. Res. Lett.* **2014**, *9* (3),

035003. https://doi.org/10.1088/1748-9326/9/3/035003.

(29) Marais, E. A.; Wiedinmyer, C. Air Quality Impact of Diffuse and Inefficient Combustion Emissions in Africa (DICE-Africa). *Environ. Sci. Technol.* **2016**, *50* (19), 10739–10745. https://doi.org/10.1021/acs.est.6b02602.

(30) Heft-Neal, S.; Burney, J.; Bendavid, E.; Burke, M. Robust Relationship between Air Quality and Infant Mortality in Africa. *Nature* **2018**, *559*, 254–258. https://doi.org/10.1038/s41586-018-0263-3.

(31) Olujimi, O. O.; Ana, G. R. E. E.; Ogunseye, O. O.; Fabunmi, V. T. Air Quality Index from Charcoal Production Sites, Carboxyheamoglobin and Lung Function among Occupationally Exposed Charcoal Workers in South Western Nigeria. *Springerplus* **2016**. https://doi.org/10.1186/s40064-016-3227-9.

(32) Tumwesige, V.; Okello, G.; Semple, S.; Smith, J. Impact of Partial Fuel Switch on Household Air Pollutants in Sub-Sahara Africa. *Environ. Pollut.* **2017**, *231*, 1021–1029. https://doi.org/10.1016/j.envpol.2017.08.118.

(33) WHO. *WHO Air Quality Guidelines for Particulate Matter, Ozone, Nitrogen Dioxide and Sulfur Dioxide: Global Update 2005: Summary of Risk Assessment*; WHO/SDE/PHE/OEH/06.02; Geneva, 2006.

(34) Wiedinmyer, C.; Yokelson, R. J.; Gullett, B. K. Global Emissions of Trace Gases, Particulate Matter, and Hazardous Air Pollutants from Open Burning of Domestic WastE. *Environ. Sci. Technol.* **2014**. https://doi.org/10.1021/es502250z.

(35) Aghedo, A. M.; Schultz, M. G.; Rast, S. The Influence of African Air Pollution on Regional and Global Tropospheric Ozone. *Atmos. Chem. Phys.* **2007**, *7* (5), 1193–1212. https://doi.org/10.5194/acp-7-1193-2007.

(36) IPCC. Guidelines for National Greenhouse Gas Inventories. *Agriculture, Forestry and*

other land use. 2006, pp 4.1-4.83. https://doi.org/10.1016/j.phrs.2011.03.002.

(37) UN. Guidelines for the 2017 United Nations Statistics Division. ANNUAL QUESTIONNAIREON ENERGY STATISTICS https://unstats.un.org/unsd/energy/Energy-Questionnaire-Guidelines.pdf (accessed Jun 4, 2019).

(38) Gathui, T. wa; Ngugi, W. *Bioenergy and Poverty in Kenya: Attitudes, Actors and Activities*; Kenya, 2010.

(39) World Bank. Population living in slums (% of urban population) https://data.worldbank.org/indicator/EN.POP.SLUM.UR.ZS (accessed Dec 15, 2018).

(40) Cadman, J.; Evans, S.; Holland, M.; Boyd, R. *Proposed Plastic Bag Levy - Extended Impact Assessment Final Report*; Scottish Executive: Edinburgh, 2005.

(41) Jagger, P.; Das, I. Implementation and Scale-up of a Biomass Pellet and Improved Cookstove Enterprise in Rwanda. *Energy Sustain. Dev.* **2018**, *46*, 32–41. https://doi.org/https://doi.org/10.1016/j.esd.2018.06.005.

(42) Huo, H.; Yao, Z.; Zhang, Y.; Shen, X.; Zhang, Q.; He, K. On-Board Measurements of Emissions from Diesel Trucks in Five Cities in China. *Atmos. Environ.* **2012**, *54*, 159–167. https://doi.org/10.1016/j.atmosenv.2012.01.068.

(43) *Energy and Development in Southern Africa*; Philip, O., Munslow, B., Eds.; Beijer Institute, Royal Swedish Academy of Sciences: Stockholm, 1984.

(44) CIESIN. Gridded Population of the World, Version 4 (GPWv4): Population Density, Revision 10 https://doi.org/10.7927/H4DZ068D (accessed Nov 12, 2018).

(45) GeoFABRIK. OpenStreetMap for Africa http://download.geofabrik.de/africa.html (accessed Jun 10, 2018).

(46) ESRI. ArcGIS Desktop: Release 10.4. *Redlands CA*. 2016.

(47) FAO. FAO GEONETWORK http://www.fao.org/geonetwork/srv/en/main.home?uuid=063720fb-79b5-44e5-832b-1c03f6b845ac (accessed May 14, 2018).

(48) UNEP-WCMC. World Database on Protected Areas https://www.protectedplanet.net/ (accessed Jan 25, 2018).

(49) Boberg, J. Competition in Tanzanian Woodfuel Markets. *Energy Policy* **1993**, *21*, 474–490.

(50) Bird, J.; Montebruno, P.; Regan, T. Life in a Slum: Understanding Living Conditions in Nairobi's Slums across Time and Space. *Oxford Rev. Econ. Policy* **2017**, *33* (3), 496–520. https://doi.org/10.1093/oxrep/grx036.

(51) Sun, S.; Jiang, W.; Gao, W. Vehicle Emission Trends and Spatial Distribution in Shandong Province, China, from 2000 to 2014. *Atmos. Environ.* **2016**, *147*, 190–199. https://doi.org/10.1016/j.atmosenv.2016.09.065.

(52) EEA. *EMEP/EEA Air Pollutant Emission Inventory Guidebook 2019. Technical Guidance to Prepare National Emission Inventories*; Luxembourg, 2019. https://doi.org/doi:10.2800/293657.

(53) USEPA. *Compilation of Air Pollutant Emissions Factors. Volume 1: Stationary Point and Area Sources*; Durham, 2009; Vol. 1.

(54) Alam, O.; Billah, M.; Yajie, D. Characteristics of Plastic Bags and Their Potential Environmental Hazards. *Resour. Conserv. Recycl.* **2018**, *132*, 121–129. https://doi.org/10.1016/j.resconrec.2018.01.037.

(55) UN. *Population 2030: Demographic Challenges and Opportunities for Sustainable*

Development Planning; 2015. https://doi.org/(ST/ESA/SER.A/389).

(56) Bailis, R.; Ezzati, M.; Kammen, D. M. Mortality and Greenhouse Gas Impacts of Biomass and Petroleum Energy Futures in Africa. *Science (80-.).* **2005**, *308* (5718), 98–103. https://doi.org/10.1126/science.1106881.

(57) Wanjiru, H.; Nyambane, A.; Omedo, G.; Davis, M.; Chelagat, W. How Kenya can transform the charcoal sector and create new opportunities for lowcarbon rural development https://www.jstor.org/stable/resrep02811 (accessed Jun 5, 2020).

(58) World Bank. Clean and improved cooking in sub-Saharan Africa. Second edition http://documents.worldbank.org/curated/en/164241468178757464/pdf/98664-REVISED-WP-P146621-PUBLIC-Box393185B.pdf (accessed Jun 5, 2020).

(59) IEA. Africa Energy Outlook 2019 https://www.iea.org/reports/africa-energy-outlook-2019 (accessed Jun 5, 2020).

(60) Mbandi, A. Air Pollution in Africa in the Time of COVID-19: The Air We Breathe Indoors and Outdoors. *Clean Air J.* **2020**, *30* (1 SE-Commentary), 1–3. https://doi.org/10.17159/caj/2020/30/1.8227.

(61) IEA. Africa and Covid-19: Economic recovery and electricity access go hand in hand https://www.iea.org/commentaries/africa-and-covid-19-economic-recovery-and-electricity-access-go-hand-in-hand (accessed Jun 5, 2020).

(62) Heald, C. L.; Ridley, D. A.; Kroll, J. H.; Barrett, S. R. H.; Cady-Pereira, K. E.; Alvarado, M. J.; Holmes, C. D. Contrasting the Direct Radiative Effect and Direct Radiative Forcing of Aerosols. *Atmos. Chem. Phys.* **2014**, *14* (11), 5513–5527. https://doi.org/10.5194/acp-14-5513-2014.

(63) Kambewa, P.; Mataya, B.; Sichinga, K.; Johnson, T. *Charcoal The Reality: A Case Study of Charcoal Consumption, Trade and Production in Malawi*; Small and Medium

Forestry Enterprise Series; 21; London, UK, 2007.

(64) Giglio, L.; Randerson, J. T.; Van Der Werf, G. R. Analysis of Daily, Monthly, and Annual Burned Area Using the Fourth-Generation Global Fire Emissions Database (GFED4). *J. Geophys. Res. Biogeosciences* **2013**, *118* (1), 317–328. https://doi.org/10.1002/jgrg.20042.

(65) Hoesly, R. M.; Smith, S. J.; Feng, L.; Klimont, Z.; Janssens-Maenhout, G.; Pitkanen, T.; Seibert, J. J.; Vu, L.; Andres, R. J.; Bolt, R. M.; Bond, T. C.; Dawidowski, L.; Kholod, N.; Kurokawa, J. I.; Li, M.; Liu, L.; Lu, Z.; Moura, M. C. P.; O'Rourke, P. R.; Zhang, Q. Historical (1750-2014) Anthropogenic Emissions of Reactive Gases and Aerosols from the Community Emissions Data System (CEDS). *Geosci. Model Dev.* **2018**, *11* (1), 369–408. https://doi.org/10.5194/gmd-11-369-2018.

(66) Guenther, A. B.; Jiang, X.; Heald, C. L.; Sakulyanontvittaya, T.; Duhl, T.; Emmons, L. K.; Wang, X. The Model of Emissions of Gases and Aerosols from Nature Version 2.1 (MEGAN2.1): An Extended and Updated Framework for Modeling Biogenic Emissions. *Geosci. Model Dev.* **2012**, *5* (6), 1471–1492. https://doi.org/10.5194/gmd-5-1471-2012.

(67) Hudman, R. C.; Moore, N. E.; Mebust, A. K.; Martin, R. V.; Russell, A. R.; Valin, L. C.; Cohen, R. C. Steps towards a Mechanistic Model of Global Soil Nitric Oxide Emissions: Implementation and Space Based-Constraints. *Atmos. Chem. Phys.* **2012**, *12* (6), 7779–7795. https://doi.org/10.5194/acp-12-7779-2012.

(68) Zender, C. S.; Bian, H.; Newman, D. Mineral Dust Entrainment and Deposition (DEAD) Model: Description and 1990s Dust Climatology. *J. Geophys. Res. Atmos.* **2003**, *108* (D14). https://doi.org/10.1029/2002JD002775.

(69) Keller, C. A.; Long, M. S.; Yantosca, R. M.; Da Silva, A. M.; Pawson, S.; Jacob, D. J.

HEMCO v1.0: A Versatile, ESMF-Compliant Component for Calculating Emissions in Atmospheric Models. *Geosci. Model Dev.* **2014**, *7* (4), 1409–1417. https://doi.org/10.5194/gmd-7-1409-2014.

(70) Park, R. J.; Jacob, D. J.; Field, B. D.; Yantosca, R. M.; Chin, M. Natural and Transboundary Pollution Influences on Sulfate-Nitrate-Ammonium Aerosols in the United States: Implications for Policy. *J. Geophys. Res. D Atmos.* **2004**, *109* (15), D15204. https://doi.org/10.1029/2003JD00473.

(71) Zhang, L.; Jacob, D. J.; Knipping, E. M.; Kumar, N.; Munger, J. W.; Carouge, C. C.; Van Donkelaar, A.; Wang, Y. X.; Chen, D. Nitrogen Deposition to the United States: Distribution, Sources, and Processes. *Atmos. Chem. Phys.* **2012**, *12* (10), 4539–4554. https://doi.org/10.5194/acp-12-4539-2012.

(72) Heald, C. L.; Jacob, D. J.; Turquety, S.; Hudman, R. C.; Weber, R. J.; Sullivan, A. P.; Peltier, R. E.; Atlas, E. L.; de Gouw, J. A.; Warneke, C.; Holloway, J. S.; Neuman, J. A.; Flocke, F. M.; Seinfeld, J. H. Concentrations and Sources of Organic Carbon Aerosols in the Free Troposphere over North America. *J. Geophys. Res. Atmos.* **2006**, *111* (D23), 1–12. https://doi.org/10.1029/2006jd007705.

(73) Wang, Q.; Jacob, D. J.; Spackman, J. R.; Perring, A. E.; Schwarz, J. P.; Moteki, N.; Marais, E. A.; Ge, C.; Wang, J.; Barrett, S. R. H. Global Budget and Radiative Forcing of Black Carbon Aerosol: Constraints from Pole-to-Pole (HIPPO) Observations across the Pacific. *J. Geophys. Res.* **2014**, *119* (1), 195–206. https://doi.org/10.1002/2013JD020824.

(74) Marais, E. A.; Silvern, R. F.; Vodonos, A.; Dupin, E.; Bockarie, A. S.; Mickley, L.; Schwartz, J. Air Quality and Health Impact of Future Fossil Fuel Use for Electricity Generation and Transport in Africa. *Environ. Sci. Technol.* **2019**, *53* (22), 13524–

13534. https://doi.org/10.1021/acs.est.9b04958.

(75) Randerson, J. T.; van der Werf, G. R.; Giglio, L.; Collatz, G. J.; Kasibhatla, P. S. Global Fire Emissions Database, Version 4.1 (GFEDv4) https://daac.ornl.gov/cgi-bin/dsviewer.pl?ds_id=1293. https://doi.org/10.3334/ORNLDAAC/1293.

(76) Lacaux, J. P.; Brocard, D.; Lacaux, C.; Delmas, R.; Brou, A.; Yoboué, V.; Koffi, M. Traditional Charcoal Making: An Important Source of Atmospheric Pollution in the African Tropics. *Atmos. Res.* **1994**, *35* (1), 71–76. https://doi.org/10.1016/0169-8095(94)90073-6.

(77) Sillman, S. The Relation between Ozone, NO(x) and Hydrocarbons in Urban and Polluted Rural Environments. *Atmos. Environ.* **1999**, *33*, 1821–1845. https://doi.org/10.1016/S1352-2310(98)00345-8.

(78) Prabamroong, T.; Manomaiphiboon, K.; Limpaseni, W.; Sukhapan, J.; Bonnet, S. Ozone and Its Potential Control Strategy for Chon Buri City, Thailand. *J. Air Waste Manag. Assoc.* **2012**, *62*, 1411–1422. https://doi.org/10.1080/10962247.2012.716385.

(79) Bond, T. C.; Streets, D. G.; Yarber, K. F.; Nelson, S. M.; Woo, J. H.; Klimont, Z. A Technology-Based Global Inventory of Black and Organic Carbon Emissions from Combustion. *J. Geophys. Res. Atmos.* **2004**, *109* (14), 1–43. https://doi.org/10.1029/2003JD003697.

(80) Jayarathne, T.; Stockwell, C. E.; Bhave, P. V.; Praveen, P. S.; Rathnayake, C. M.; Md Islam, R.; Panday, A. K.; Adhikari, S.; Maharjan, R.; Douglas Goetz, J.; Decarlo, P. F.; Saikawa, E.; Yokelson, R. J.; Stone, E. A. Nepal Ambient Monitoring and Source Testing Experiment (NAMaSTE): Emissions of Particulate Matter from Wood-and Dung-Fueled Cooking Fires, Garbage and Crop Residue Burning, Brick Kilns, and Other Sources. *Atmos. Chem. Phys.* **2018**, *18* (3), 2259–2286.

https://doi.org/10.5194/acp-18-2259-2018.

(81) Pennise, D. M.; Smith, K. R.; Kithinji, J. P.; Rezende, M. E.; Raad, T. J.; Zhang, J.; Fan, C. Emissions of Greenhouse Gases and Other Airborne Pollutants from Charcoal Making in Kenya and Brazil. *J. Geophys. Res. Atmos.* **2001**, *106* (D20), 24143–24155. https://doi.org/10.1029/2000JD000041.

(82) Ekeh, O.; Fangmeier, A.; Müller, J. Quantifying Greenhouse Gases from the Production, Transportation and Utilization of Charcoal in Developing Countries: A Case Study of Kampala, Uganda. *Int. J. Life Cycle Assess.* **2014**, *19* (9), 1643–1652. https://doi.org/10.1007/s11367-014-0765-7.

(83) Andela, N.; Van Der Werf, G. R. Recent Trends in African Fires Driven by Cropland Expansion and El Niño to La Niña Transition. *Nat. Clim. Chang.* **2014**, *4* (9), 791–795. https://doi.org/10.1038/nclimate2313.

(84) Duncan, B. N.; West, J. J.; Yoshida, Y.; Fiore, A. M.; Ziemke, J. R. The Influence of European Pollution on Ozone in the Near East and Northern Africa. *Atmos. Chem. Phys.* **2008**, *8* (8), 2267–2283. https://doi.org/10.5194/acp-8-2267-2008.

(85) Tyson, P. D.; Garstang, M.; Swap, R. Large-Scale Recirculation of Air over Southern Africa. *J. Appl. Meteorol.* **1996**, *35* (12), 2218–2236. https://doi.org/10.1175/1520-0450(1996)035<2218:LSROAO>2.0.CO;2.

(86) Leah Laban, T.; Gideon Van Zyl, P.; Paul Beukes, J.; Vakkari, V.; Jaars, K.; Borduas-Dedekind, N.; Josipovic, M.; Mee Thompson, A.; Kulmala, M.; Laakso, L. Seasonal Influences on Surface Ozone Variability in Continental South Africa and Implications for Air Quality. *Atmos. Chem. Phys.* **2018**, *18* (20), 15491–15514. https://doi.org/10.5194/acp-18-15491-2018.

(87) Vodonos, A.; Awad, Y. A.; Schwartz, J. The Concentration-Response between Long-

Term $PM_{2.5}$ Exposure and Mortality; A Meta-Regression Approach. *Environ. Res.* **2018**, *166*, 677–689. https://doi.org/10.1016/j.envres.2018.06.021.

(88) Marais, E. A.; Jacob, D. J.; Wecht, K.; Lerot, C.; Zhang, L.; Yu, K.; Kurosu, T. P.; Chance, K.; Sauvage, B. Anthropogenic Emissions in Nigeria and Implications for Atmospheric Ozone Pollution: A View from Space. *Atmos. Environ.* **2014**, *99*, 32–40. https://doi.org/10.1016/j.atmosenv.2014.09.055.

(89) Saunois, M.; Reeves, C. E.; Mari, C. H.; Murphy, J. G.; Stewart, D. J.; Mills, G. P.; Oram, D. E.; Purvis, R. M. Factors Controlling the Distribution of Ozone in TheWest African Lower Troposphere during the AMMA (African Monsoon Multidisciplinary Analysis) Wet Season Campaign. *Atmos. Chem. Phys.* **2009**, *9*, 6135–6155. https://doi.org/10.5194/acp-9-6135-2009.

(90) Naik, V.; Mauzerall, D. L.; Horowitz, L. W.; Schwarzkopf, M. D.; Ramaswamy, V.; Oppenheimer, M. On the Sensitivity of Radiative Forcing from Biomass Burning Aerosols and Ozone to Emission Location. *Geophys. Res. Lett.* **2007**, *34*, L03818. https://doi.org/10.1029/2006GL028149.

(91) Mickley, L. J.; Murti, P. P.; Jacob, D. J.; Logan, J. A. Radiative Forcing from Tropospheric Ozone Calculated with a Unified Chemistry-Climate Model. *J. Geophys. Res. Atmos.* **1999**, *104* (D23), 30153–30172. https://doi.org/10.1029/1999JD900439.

(92) Jaeglé, L.; Jacob, D. J.; Wang, Y.; Weinheimer, A. J.; Ridley, B. A.; Campos, T. L.; Sachse, G. W.; Hagen, D. E. Sources and Chemistry of NO_x in the Upper Troposphere over the United States. *Geophys. Res. Lett.* **1998**, *25*, 1705–1708. https://doi.org/10.1029/97GL03591.

(93) Dahlmann, K.; Grewe, V.; Ponater, M.; Matthes, S. Quantifying the Contributions of Individual NO_x Sources to the Trend in Ozone Radiative Forcing. *Atmos. Environ.*

2011, *45* (17), 2860–2868. https://doi.org/10.1016/j.atmosenv.2011.02.071.

(94) Unger, N.; Shindell, D. T.; Koch, D. M.; Streets, D. G. Air Pollution Radiative Forcing from Specific Emissions Sectors at 2030. *J. Geophys. Res. Atmos.* **2008**, *113* (2), D02306. https://doi.org/10.1029/2007JD008683.

(95) Bolognesi, M.; Vrieling, A.; Rembold, F.; Gadain, H. Rapid Mapping and Impact Estimation of Illegal Charcoal Production in Southern Somalia Based on WorldView-1 Imagery. *Energy Sustain. Dev.* **2015**, *25*, 40–49. https://doi.org/https://doi.org/10.1016/j.esd.2014.12.008.